

NASDA Activities in Space Solar Power System Research, Development and Applications

Sumio MATSUDA, Yasunari YAMAMOTO, Masato UESUGI
TSUKUBA SPACE CENTER, NASDA¹

Abstract

This paper describes NASDA activities in solar cell research, development and applications. First, we review current technologies for space solar cells such as Si, GaAs and InP. Second, we discuss future space solar cell technologies intended to be used on satellites of 21st century. Next, we show the flight data of solar cell monitor on ETS-V. Finally, we propose to establish the universal space solar cell calibration system.

1. Introduction

Solar cells have been a dependable power source for use in space for the last 30 years, and have served as the primary power source for satellites. The performance of Si solar cells has increased from 10% air mass zero (AM0) solar energy conversion efficiency in the early 1960s to almost 15% on today's spacecraft. However, as larger satellites with greater output and longer life are developed, their power supplies will strongly require solar cells with higher efficiency, lighter weight, and longer life to increase the specific power (W/Kg) and the areal power density (W/m²) of the solar array. Reduction of solar array mass is especially important for high earth altitude or geosynchronous orbit missions due to launch vehicle cost and a restricted launch vehicle capability to boost payloads into high earth orbit. In addition, a reduction in solar array mass and/or increase in specific power enables a greater allocation for more sensors, transponders, or additional payload on existing spacecraft. Furthermore, higher areal power densities are important for low-altitude earth orbit due to the environmental drag on the surface of the solar array, causing altitude adjustments with an auxiliary reactor control gas thruster subsystem and decreasing the fuel supply and mission life.

Gallium Arsenide (GaAs) and Indium Phosphide (InP) solar cells have been expected to supplant Si solar cells because of their high efficiency and high radiation tolerance. GaAs solar cells were adopted for main solar arrays to satisfy the requirement Japanese domestic communications satellites (CS-3), which were successfully launched in 1988 and have been generating almost the expected power. Meanwhile InP solar cells are also being used as a photovoltaic power

source with output power of 10-20 watts on the lunar mission of the Japanese scientific satellite MUSES-A, which was launched in January 1990 by Institute of Space and Astronautical Science.

The photovoltaic element of the space energy conversion programs designed to provide the technology for efficiency improvement, mass and cost reduction, and operating life extension for solar cells and arrays. This paper describes the state of the technology of advanced solar cells for space applications.

2. Technology for Space Solar Cells

The status and trends in development of several kinds of solar cells for space use are shown in Table 1. Here, the status of production and technology for Si, GaAs, and InP solar cells, which are currently available for space use, are introduced.

2.1 Si Solar Cells

(1) Thin Si solar cells

Thin silicon solar cells have the advantages of lighter weight and higher radiation resistance than conventional thick (200 μ m) solar cells. Since the development of 50 μ m thin silicon solar cells in 1983, the thin solar cells have been used for Japanese satellite programs, ERS-1, ETS-VI and ADEOS of NASDA. (see Table 2)

(2) Improvement of thin solar cells

To meet the requirement of high efficiency from solar array side, the electrical performance of the thin solar cells was improved in 1990 by introducing fine gridlines forming method which used the photolithographic masks and lift off technique. The gridlines of the former cells were formed by evaporation through the metallic masks. The gridlines through metallic masks were minimum 20 μ m wide and 1mm spacing. The gridline penumbra originated from small gaps between metallic masks and silicon surfaces was

¹2-1-1 SENGEN, TSUKUBA-SHI IBARAKI-KEN 305 JAPAN

5 to 20µm wide and caused output current loss. The improved new cells showed about 6% higher output power than the former cells. The characteristics and electrical performance of the new cells are given in Table 3. The 4cmx6cm thin silicon solar cells were newly fabricated from the 4 inch silicon wafer process.

The qualification tests and characterization of the thin solar cells were performed according to NASDA specification, NASDA-QTS-1013 and they satisfied all test requirements. The production of the improved solar cells (about 60000 2cmx4cm 100µm thick CIC's) started for ADEOS program in 1991.

Table 1 Status and trends in solar cells for space applications

Solar Cell		Current	Goal or trend
Si	In Production	13% to 15%	High power to weight ratio Low cost
	Efficiency		
	Size/Thickness	4x6cm/50µm	Large Area/Light Weight
	In development	17.5% efficiency (2x2cm)	High efficiency(20%)
GaAs	In production	18% to 20%	Light weight concentrator
	efficiency		
	Size/Thickness	2x4cm/200µm	
InP	In pilot- production	16% to 17%	Higher efficiency(20%) Low cost
	efficiency	(1x2cm)	
GaAs on Si	In development	18%	Higher efficiency
	efficiency	(2x2cm)	Light weight

* Conversion Efficiency is for AM0

Table 2 Solar Cell Applications of NASDA Satellite

	ETS-V	CS-3a CS-3b	GMS-4	MOS-1b	BS-3a BS-3b	JERS-1	ETS-VI	GMS-5	ADEOS	COMETS
Launch Date	87.8.27	88.2.19 88.9.16	89.9.6	90.2.7	90.8.28 91.2.25	92.2.11	94 SUMMER	95 WINTER	96 WINTER	97 WINTER
Satellite Shape	Box	Cylindrical	Cylindrical	Box	Box	Box	Box	Cylindrical	Box	Box
Satellite Weight	550kg	550kg	325kg	740kg	550kg	1340kg	2000kg	345kg	3500kg	2000kg
Satellite Life	1.5y	7y	5y	2y	7y	2y	10y	5y	3y	3y
Satellite Power (EOL)	845W	628W	265W	540W	1482W	2053W	4100W	-	4500W	5400W
Solar Cell Type	Si BSFR	GaAs	Si BSFR	Si BSF	Si BSR	Si BSFR	Si BSFR	Si BSFR	Si BSFR	GaAs
Solar Cell Size	2cmx4cm	2cmx2cm	6.2cmx2.2cm ^{*1} 2cmx2cm	2cmx4cm	2cmx4cm	2cmx4cm	2cmx4cm	2.43cmx 6.2cm	2cmx4cm	2cmx4cm
Solar Cell Thickness	280µm	280µm	200µm ^{*1} 280µm ^{*2}	280µm	200µm	50µm	50µm	200µm	100µm	200µm
Cover-glass	CMX150	CMS150	OCLI 150µm	CMS150	OCLI 150µm	AS100	AS50	OCLI 150µm	AS100	AS100

*1: main array
*2: charge array

The 4 inch diameter, CZ, (100) oriented, 200 μ m thick, chemically polished silicon wafers were etched to the target thickness in a hot sodium hydroxide solution. The fine gridlines on the surface were formed by the photolithography technique. The outline of fabrication process is shown below.

1. Thinning etch
2. Texturing etch (formation of NRS)
3. Passivation of rear surface
4. p and n diffusion
5. Contact formation
6. A.R.C. formation
7. Cutting to 2cmx2cm

(2) Experimental Results

The electrical performance data of the solar cells are shown in Table 5. The 100 μ m thick solar cells with random pyramid surface showed the highest efficiency (17.5%) of all cells. The electrical parameters at the operating temperature were also calculated from the energy balance equation of the flat solar cell array considering the solar absorptance (α_s : measured values in Table 5) and the hemispherical emittance (ϵ_n :0.80) of the solar cell and the hemispherical (ϵ_n : 0.80) of rear surface of the array substrate. The V-groove cells showed higher power at the operating temperature due to their low solar absorptance (0.77-0.79) than the other solar cells.

The spectral reflectance of the 50 μ m thick solar cell with three types of NRS is shown in Fig. 2. The V-groove cell showed the highest reflectance in the infrared spectrum (1100nm-2500nm) and gave the lowest solar absorptance (0.77). The inverted pyramid cell showed intermediate reflectance in the infrared spectrum. The random pyramid cell showed the lowest reflectance for whole wavelength range and generated the highest power of all the cells.

The random pyramid cells were irradiated by 1MeV electrons to 3×10^{15} e/cm². Degradation curves of maximum power of 50 μ m, 70 μ m and 100 μ m thick solar cells are shown in Fig.3. After electron irradiation to more than 1×10^{16} e/cm², thinner cells showed higher Pmax similarly as the conventional BSFR cells with the whole area BSF layer and the back surface reflector (BSR) of aluminum thin layer and without the NRS and passivated rear surface. Degradation rates of the high efficiency solar cells were a little higher than those of the conventional BSFR cells, but absolute Pmax values after electron irradiation were fairly larger than those of the conventional BSFR cells.

From these data, we think that thin (50 μ m, 70 μ m and 100 μ m) silicon solar cells with nonreflective surface (NRS), passivated rear surface and locally diffused p BSF layer are hopeful candidates for space applications.

Table 5 Electrical performance of high efficiency thin silicon solar cells

NRS	Configuration of Solar Cell			Electrical Performance at 28°C					α_s	Performance at Top		
	Resistivity (Ω cm)	Thickness (μ m)	BSF	Voc(mV)	Isc(mA)	Pmax(mW)	Fill Factor	Efficiency		Top	Pmax(mW)	Efficiency
										(°C)	@ Top	@ Top
RANDOM	10	50	localized	633.0	188.4	93.0	0.790	17.2%	0.85	45.2	86.5	16.0%
		70		629.0	191.6	93.7	0.794	17.3%	0.85	45.6	87.0	16.1%
		100		628.0	193.1	94.6	0.785	17.5%	0.86	46.8	87.5	16.2%
INVERTED	10	50	localized	641.0	180.7	90.2	0.787	16.7%	0.80	39.2	86.1	15.9%
		70		630.0	186.4	91.6	0.791	16.9%	0.82	41.8	86.5	16.0%
		100		632.0	188.4	93.2	0.784	17.2%	0.83	42.8	87.6	16.2%
V-GROOVE	10	50	localized	634.0	181.8	89.7	0.795	16.6%	0.77	36.2	86.8	16.0%
		70		630.0	185.8	91.3	0.790	16.9%	0.78	37.0	88.1	16.3%
		100		629.0	186.3	91.3	0.784	16.9%	0.79	37.4	87.8	16.2%
without NRS	10	50	whole	605.0	160.0	76.5	0.790	14.1%	0.75	36.3	73.9	13.7%
		70		605.0	163.0	78.0	0.791	14.4%	0.75	35.9	75.6	14.0%
		100		605.0	166.0	79.5	0.792	14.7%	0.76	36.9	76.7	14.2%

Note. Cell Dimensions : 20 x 20 mm

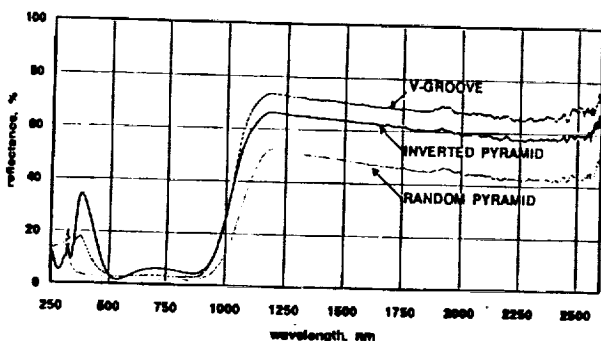


Fig. 2 Spectral reflectance of solar cells

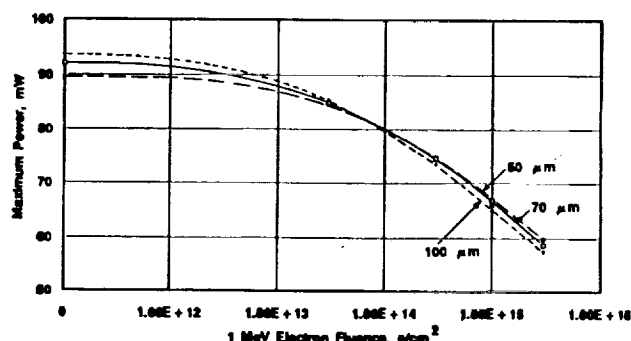


Fig. 3 Degradation curves of Pmax of the 50 μ m, 70 μ m and 100 μ m thick random pyramid cells.

Table 3 Cell Electrical Parameter

Solar Cell Type	200 μ m BSR (2 Ω cm)	200 μ m BSR (10 Ω cm)	100 μ m BSFR	70 μ m BSFR	50 μ m BSFR
Open Circuit Voltage(V_{oc}), mV	592	548	610	610	610
Short Circuit Current(J_{sc}), mA/cm ²	40.0	40.0	42.2	41.4	40.7
Cell Load Voltage(V_L), mV	490	450	500	500	500
Cell Load Current(J_L), mA/cm ²	38.1	38.1	40.2	39.5	38.7
Cell Power(P), mW/cm ²	18.7	17.1	20.2	19.8	19.4
Efficiency(η), %	13.8	12.7	14.9	14.6	14.3

Note : Measuring Conditions ; Cell Temperature 28°C,
AMO 135.3mW/cm²

2.2 GaAs solar cells

GaAs solar cells have been expected to serve as future space power sources because of high efficiency, high radiation tolerance, and ability to operate at high temperature. High efficiency GaAs solar cells with an average efficiency of 18.9% at AMO have been obtained by liquid phase epitaxy (LPE), and AMO efficiency as high as 22.5% has been reported by using metalorganic chemical vapor deposition (MOCVD). As mentioned above, GaAs solar cells were adopted as primary power sources for Japanese communications satellites, which were successfully launched in 1988, and the cells have been generating nearly the expected power. The flight data of CS-3 have proved that radiation damage to a GaAs solar cell is less than that of a Si solar cell (thickness is over 200 μ m). The production of the improved GaAs solar cells (about 40,800 2cmx4cm 200 μ m thick) started for COMETS program in 1992. This is thought to stem from differences in the optical-absorption and photocarrier generation mechanism of GaAs and Si: in GaAs the diffusion length is sufficiently large compared with the thickness of the region where most of the photo-carriers are produced, and the junction depth of 0.5 \pm 0.1 μ m is shallow, so damage is small and degradation of the diffusion length is slight, resulting in little drop in the efficiency. While the diffusion length in silicon is comparable with the thickness of the active region, the efficiency decreases with the decrease of diffusion length.

GaAs solar cells with 18% to 20% efficiency, 2cmx4cm in size and 200 μ m in thickness, have been fully qualified for space use and are being mass-produced. This cell has the AlGaAs/GaAs heteroface structure, which

consists of p-AlGaAs/p-GaAs/n-GaAs buffer layer/n-GaAs substrate. This type of heteroface AlGaAs/GaAs solar cell can be produced by the liquid phase epitaxy process named VSTC-LPE. CS-3 solar array is covered with 36,671 2cmx2cm GaAs solar cells.

2.3 InP solar cells

Recently, much effort has been devoted to the study of InP solar cells for space applications owing to the radiation resistance and annealing properties of InP. The radiation resistance of InP solar cells are superior to that of GaAs or Si solar cells under 1 MeV electron and 10 MeV proton irradiation. Furthermore, the degradation can be removed by annealing at a relatively low temperature.

As mentioned above, 1300 pieces of 2cmx1cm InP solar cells with AMO efficiency of 16% to 17% were used as the power source of a satellite for a lunar mission. These cells have a n/p homojunction of InP, which was formed by diffusing sulfur into p-type substrates.

One obstacle to the production of InP solar cells is the high cost of the InP substrate. For this reason much effort has been devoted to work on heteroepitaxy such as InP-on-Si and to the CLEFT (Cleavage of Lateral Epitaxial Films for Transfer) process for removal and recovery of the substrate.

3. Future space solar cell technology

Solar arrays are expected to become larger in area, lighter in weight, and longer-lived. In addition, the cost/watt of such solar arrays needs to be decreased from the present level. Major advances in the performance and fabrication technology for solar cells

must be made in order to meet the above broad system needs. The main areas of activity for solar cells for space applications in the near future fall into the following three categories:

3.1 Si high efficiency solar cells

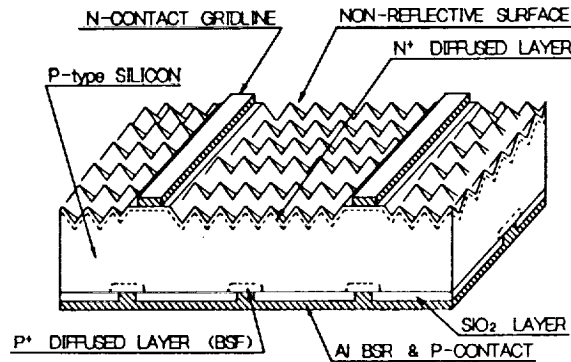
The first research program to improve thin silicon solar cell performance (target efficiency: 17% on 100 μ m cell) started in November 1990. Main aim of this program was a basic research of high efficiency thin solar cells for future spacecraft. After completion of this program in April of 1992, the second research program (target efficiency: 18% on 100 μ m cell) started in June of this year. The

qualification test program of the high efficiency thin silicon solar cells for space application will be performed in the next fiscal year.

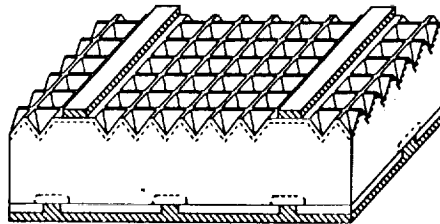
The basic design of the solar cell with nonreflective surface (NRS), passivated rear surface and locally P' diffused BSF layer was confirmed to be very effective for improving characteristics of the space solar cells.

(1) Cell design and process

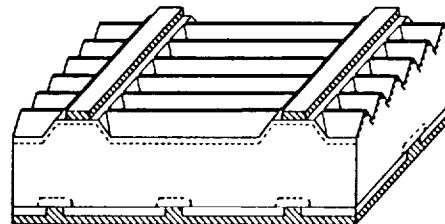
Three types of NRS (normal pyramid, inverted pyramid and V-groove) and the above basic design as shown in Figure 1. The main features of these thin solar cells are given in Table 4.



(a) Random Pyramid



(b) Inverted Pyramid



(c) V-groove

Figure 1 Solar cell structure with various NRS.

Table 4 Main features of high efficiency thin silicon solar cells

Item	Feature
Cell dimension	- 2cmx2cm
Cell thickness	- 50 μ m, 70 μ m and 100 μ m
Substrate	- CZ, P type, 10 Ω cm
Surface	- NRS (normal pyramid, inverted pyramid and V-groove)
PN junction	- Shallowly diffused with phosphorous ($X_j=0.15\mu$ m)
Rear P' layer	- Locally diffused with boron
Passivation	- Rear surface passivation by SiO ₂
N contact	- Ti-Pd-Ag
P contact	- Al-Ti-Pd-Ag
A.R. Coating	- Dual layer coating

In addition to the high efficiency, the solar cell structure which enables prevention of an accident caused by a reverse bias has been proposed. When a part of solar cell array is shadowed, shadowed submodule are reverse biased. If the reverse bias voltage is higher than the breakdown reverse bias voltage is higher than the breakdown voltage of the cell, breakdown of cell submodule occurs and may results in permanent failure of the module. "The solar cell with bypass diode operation" has a structure in which a breakdown due to the reverse bias voltage is less liable to occur. Fig. 4 shows an equivalent circuit of this cell. The cell is connected in parallel with a diode which has plural small P⁺N⁺ junctions. This can prevent a permanent failure of the solar cell. Fig. 5 shows one of the structures of this ideas.

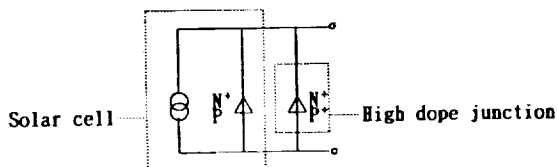


Fig.4 Equivalent circuit of the solar cell with bypass diode operation

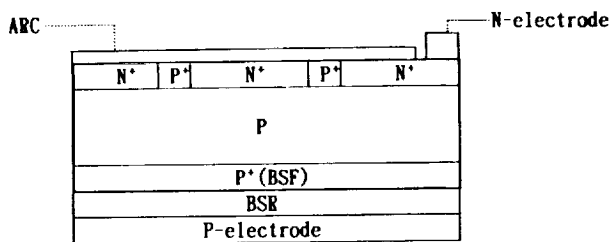


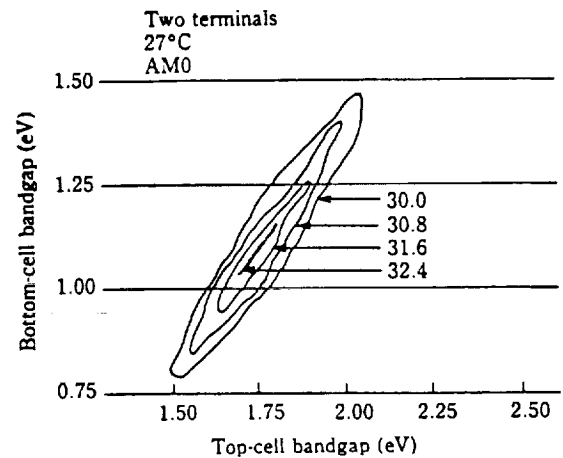
Fig.5 One of the structures of the solar cell with bypass diode operation

3.2 Thin film GaAs solar cells

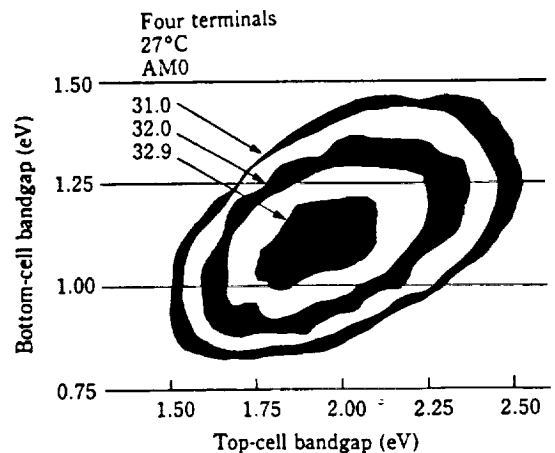
Since the optical absorption coefficient of GaAs is large, GaAs solar cells are generally able to minimize material cost without degrading efficiency. They are on-going either by the CLEFT process or by fabricating GaAs solar cells on substrate such as silicon. The GaAs-on-Si solar cells are expected to provide low weight, low cost and large area, and an efficiency rate of 18.3% has been obtained by combining in-situ thermal cycling and strained superlattices in the laboratory. However, there are problems with lattice mismatch and the thermal expansion coefficient between GaAs and Si. Emphasis should be placed on developing techniques for assembling thin GaAs for the CLEFT process and the crystal growth technique of high quality GaAs on Si substrate for the GaAs-on-Si solar cell.

3.3 Multi-junction solar cells

Substantial efficiency increases are expected for two-cell tandem structures in comparison with single-junction cells. Figure 6 shows the efficiency contour map of a two-junction tandem solar cell in a two-terminal and a four-terminal configuration. The maximum theoretical efficiency is 32.4% at AM0 for a two-terminal and 32.9% at AM0 for a four-terminal. The top cell should have an energy gap of 1.7 to 1.8 eV and the bottom cell should have a gap of about 1.0 to 1.1 eV. The top cell could be fabricated from Al_{0.5}Ga_{0.5}As or Ga_{0.5}PAs. The bottom cell of a Si cell will be utilized for economic reasons.



(a) AMO iso-efficiency plots for the two-cell, two-terminal tandem structure at 27°C and one sun (J.C.C. Fan et al.)



(b) AMO iso-efficiency plots for the two-cell, four-terminal tandem structure at 27°C and one sun (J.C.C. Fan et al.)

Fig.6

A two-terminal cell requires current matching between the top and bottom cells for optimum performance. Anything which causes current mismatch,

such as radiation damage, will lead quickly to degraded total performance. In a four-terminal configuration two cells are electrically independent of each other, so that the effect will not be compounded as rapidly. Complexity will increase at the array level, however, because essentially two power conditioning circuits must be employed. The presumption is that the increased performance will be worth the extra effort.

4. Solar Cell Monitor on ETS-V

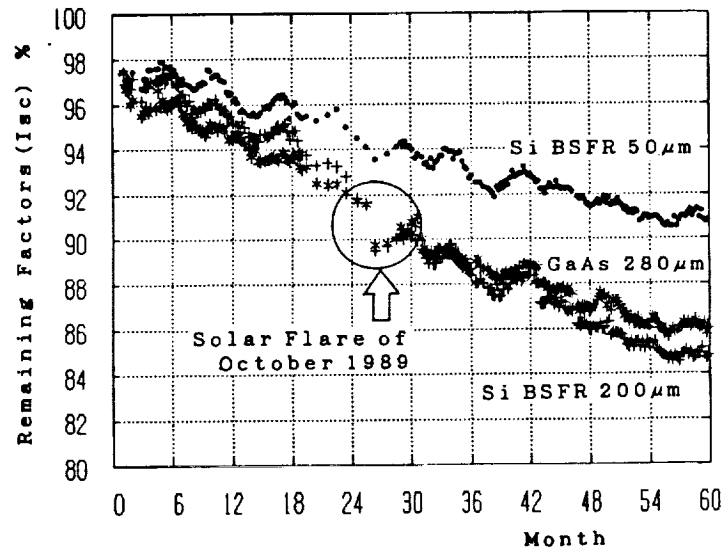
NASDA had launched Engineering Test Satellite-V (ETS-V) on 27 August 1987 and had put it into a geostationary orbit at longitude 150 degrees east. This satellite has the technical Data Acquisition Equipment (TEDA) to obtain technical data for developing satellites. The TEDA consists of 8 monitors and one of them is Solar Cell Monitor(SCM).

In the sensor parts of SCM, 24 solar cells are attached to Aluminum panels.

These cells differ in the cell thickness, cell structure, growth method of epitaxial layer, cover glass thickness and cell material (GaAs and Si) so as to investigate the effects of these parameters. In SCM the generated currents and voltages are measured on ten load conditions for each cell. Fig.7 shows the flight data of remarkable three cells which are GaAs LPE cell, Si BSFR 200 μ m and Si BSFR 50 μ m after correction. Observation data must be corrected because of following reasons.

- (1) incident solar power correction
- (2) angle correction
- (3) temperature correction

On 27 August 1992 (5 years after launched) the remaining factors of GaAs, Si BSFR 200 μ m and Si BSFR 50 μ m are about 86%, 85% and 91% respectively. These data also show degradation by solar flare of 19 October 1989.



(The day of origin = August 27, 1987)
 Fig.7 The Flight Data of Remarkable Three Cells

5. Universal Space Solar Cell Calibration System

(1) Background

From the design of the space solar cell to the assemble of the array, it is necessary to high accuracy measurement of the solar cell performance. Small errors in measuring solar cell performance and its variation due to the effects of temperature and radiation damage can be significant to a solar array designer or manufacturer. Poor estimates of solar cell performance can lead to incorrect power estimates and as a result errors in optimizing costs and mass.

When testing a large variety of

space solar cells of different types and from various manufacturers of solar cell, it is necessary to choose with some care the standard against which the cell be calibrated in AMO condition.

The solar cells can be tested on the ground, in a balloon, in a high altitude aircraft or on board of a free-flying satellite. The satellite calibration is more complete than any of the other, suffering only one disadvantage; the test article cannot be recovered.

We are now thinking about the possibility to establish a standard universal calibration system of space solar cells, the outdoor calibration method of reference solar cells (Global

Sunlight Method) for terrestrial application, and the measurement method of solar modules with the calibrated reference solar cells by developing stable solar simulators and precise spectro-radiometers.

We suggest the following items to be carried out this year as the first step:

To identify the difference between each calibration system of NASA/JPL, NASA/Lewis, CNES, and NASDA, we will provide some Si solar cells to each facility with electrical data obtained by the our solar simulator. The cells will be calibrated by each facility using their usual calibration method. The calibrated values will be compared with each other quantitatively and the difference will be discussed to establish a good standard method next year.

(2) Proposed Plan of Round Robin Calibration

The purpose of this proposed plan which is to compare "the calibrated value by Indoor Calibration Method" with "the calibrated value by Balloon Flight or Aircraft Calibration". By using the calibration results, we would like to confirm which AMO condition (WMO, Johnson, Neckel & Labs, Thekaekara and so on) is preferable.

We compare the results of Indoor Calibration Method (Solar Simulator Method) with Balloon Flight & Aircraft Calibration Method respective which AMO (WMO, Johnson, Neckel & Labs, Thekaekara and so on) is preferable by the Indoor Calibration Method. We send back the results of comparison to each calibration facilities.

6. Conclusion

We can reach that efficiency of Si solar cells become 17-18%. Next target is a large area solar cell such as 8cmx8cm or 10cmx10cm, on condition that thickness is less than 100 μ m. We will try that GaAs and InP solar cells are planned to thin film on Si or Ge on this century. Next, we will plan to carry TEDA on satellites of NASDA development. We will collect the flight data about space radiation environment and this data will be useful for satellite design. We would like to establish the universal space solar cell calibration system similar to ground solar cell calibration system. We believe 21st century is era of solar power system.

NASDA will continue to develop new solar cells for space applications in the future.

References

[1] S.Yoshida and S.Matsuda, Optoelectronics Devices and Technologies (1990) 285

[2] S.Yoshida, N.Imura, M.Goto, and S.Matsuda, Proc.4th European Symp. Photovoltaic Generators in Space (1984)65.

[3] S.Matsuda, S.Yoshida, and A.Kawakami, Proc.5th European Symp. Photovoltaic Generators in Space (1986)31.

[4] M.Yamaguchi, C.Uemura, A.Yamamoto, and A.Shibukawa, Jpn.J.Appl. Phys.,23(1984)302.

[5] L.Weinberg,C.K.Swartz,and R.E.Hart,Jr.,Proc.18th IEEE Photovoltaic Specialists Conf.(1985).

[6] S.Yoshida, H.Matsumoto, M.Goto, M.Ohmura, N.Takata, H.Kurahata, S.Matsuda,and T.Okuno,Proc.21th IEEE Photovoltaic Specialists Conf.(1990),(to be published).

[7] M.Yamaguchi, T.Hayashi, A.Ushirokawa, Y.Takahashi, M.Koubata, M.Hashimoto, and H.Okazaki, Proc.21th IEEE Photovoltaic Specialists Conf.(1990)

[8] S.Yoshida, H.Matsumoto, K.Sato, S.Hokuyo, M.Ohkubo, and S.Matsuda, AIAA 12th International Satellite Syst. Conf.(1988)63.

[9] S.Matsuda, H.Matsumoto, S.Hokuyo, and S.Yoshida, Proc.3rd Int'l. PVSEC Tokyo(1987)191.

[10] S.Yoshida, H.Matsumoto, M.Okubo, and Y.Okawa, Proc. European Space Power Conf.(1989)623.

[11] M.Yamaguchi,Proc.20th IEEE Photovoltaic Specialists Conf.(1988)880.

[12] H.Okazaki, T.Takamoto, H.Takamura, T.Kamei, M.Ura, A.Yamamoto, and M.Yamaguchi, Proc.20th IEEE Photovoltaic Specialists Conf.(1988)886.

[13] J.C.C.Fan, Proc.15th IEEE Photovoltaic Specialists Conf.(1981)666.

[14] H.Ohmachi,T.Ohhara, and Y.Kadota, Proc.21th IEEE Photovoltaic Specialists Conf.(1990).

[15] H.Okamoto, Y.Kadota, Y.Watanabe, Y.Fukuda, T.Ohhara, and Y.Ohmachi, Proc.20th IEEE Photovoltaic Specialists Conf.(1988)475.

[16] J.C.C.Fan, B.Y.Tsaur, and B.J.Palm, Proc.15th IEEE Photovoltaic Specialists Conf.(1982)692.

[17] S.Matsuda et al, Proceeding of the European Space Power Conference, (1991) 609

[18] M.Uesugi et al, Proceeding of the 22nd IEEE Photovoltaic Specialists Conference,(1991)1521

[19] T.Katsu et al, 18th International Symposium on Space Technology and Science (ISTS), Kagoshima, Japan,May 18,1992

[20] H.Washio et al, 11th European Solar Energy Conference, Oct.13, 1992